Comparison of Hydrogen Atom Abstraction Rates of Terminal and Bridging Hydrides in Triosmium Clusters: Absolute Abstraction Rate Constants for Benzyl Radical

James A. Franz,*,[†] Douglas S. Kolwaite,[†] John C. Linehan,[†] and Edward Rosenberg*,[‡]

Pacific Northwest National Laboratory, Richland, Washington 99352, and Department of Chemistry, University of Montana, Missoula, Montana 57812

Absolute rate constants for hydrogen atom abstraction by benzyl radical from $Os_3(\mu\text{-}H)_2(CO)_9PPh_3$ (**1**), $Os_3(\mu\text{-}H)(H)(CO)_{10}PPh_3$ (**2**), $Os_3(\mu\text{-}H)(CO_9)(\mu_3\text{-}\eta^2\text{-}C_9H_6N)$ (**3**), $Os_3(\mu\text{-}H)(CO_9)(\mu\text{-}\eta^2\text{-}C_9H_6N)(PPh_3)$ (**4**), and $Os_3(\mu\text{-}H)(CO_{10})(\mu\text{-}\eta^2\text{-}C_9H_6N)$ (**5**) were determined in benzene by competition of the abstraction reaction with the self-termination of benzyl radical. Thus, experimental values of $k_{abs}/k_t^{1/2}$ were combined with rate constants for self-termination of benzyl radical in benzene from the expression $\ln(2k_t/M^{-1}\ s^{-1} = 27.23 - 2952.4/RT)$, RT in cal/mol, to give absolute rate constants for abstraction, k_{abs}: for $Os_3(\mu\text{-}H)_2(CO)_9PPh_3$ (**1**) in benzene, $\log(k_{abs}/M^{-1}\ s^{-1}) = (9.40 \pm 0.30) - (8.11 \pm 0.47)/\theta$; for $Os_3(\mu\text{-}H)(H)(CO)_{10}PPh_3$ (**2**) $\log(k_{abs}/M^{-1}\ s^{-1}) = (8.08 \pm 0.33) - (4.32 \pm 0.1)/\theta$; for $Os_3(\mu\text{-}H)(CO)_9(\mu_3\text{-}\eta^2\text{-}C_9H_6N)$ (**3**) $\log(k_{abs}/M^{-1}\ s^{-1}) = (10.1 \pm 2) - (10.5 \pm 3)/\theta$; and for $Os_3(\mu\text{-}H)(CO_9)(\mu\text{-}\eta^2\text{-}C_9H_6N)(PPh_3)$ (**5**) $\log(k_{abs}/M^{-1}\ s^{-1}) = (7.0 \pm 0.27) - (4.25 \pm 0.41)/\theta$, $\theta = 2.303RT$ kcal/mol. The terminal hydride on the Os_3 cluster **2** is about 10 times more reactive than the bridging hydride in **1**. The results show that while $\mu\text{-}H$ bridging retards the rate of hydrogen abstraction relative to terminal hydrogen, the bridging hydrogen remains appreciably reactive in the $\mu\text{-}H$ form. In fact, one of the fastest rates observed was for the bridging hydride in **4**, $Os_3(\mu\text{-}H)(CO_{10})(\mu\text{-}\eta^2\text{-}C_9H_6N)$. The 293 K rate constant for hydrogen atom abstraction from this electron-rich cluster, $5 \pm 2 \times 10^4\ M^{-1}\ s^{-1}$, is almost as fast as that for the terminal hydrogen atom cluster, **2**, $Os_3(\mu\text{-}H)(H)(CO)_{10}PPh_3$, $k_{abs}(298\ K) = 8.2 \times 10^4\ M^{-1}\ s^{-1}$. The rate constant for hydrogen atom abstraction by benzyl radical from the Os_3 clusters appears to increase with electron-rich osmium clusters and decrease with increasing steric bulk of the ligands.

Introduction

The fundamental properties of hydrogen transfer from transition metals are of widespread interest due to the importance of proton, hydrogen atom, and hydride transfer in stoichiometric and catalytic systems.[1] However, the homolytic reactivity of metal hydrides in bonding arrangements found in metal clusters, such as a hydrogen atom in μ-bonds between adjacent metals, has received little study. Hydrogen abstraction from metals by carbon-, heteroatom-, and main group metal-centered radicals during radical-mediated reduction reactions is important to the understanding of numerous reaction systems.[2] The μ-H bonding mode is related to forms of hydrogen bound to metal surfaces. Several studies have developed qualitative evidence for carbon-centered radical attack on bridging and terminal hydrides.[3] The cluster $(\mu\text{-}H)_2Os_3(CO)_{10}$, possessing two

bridged hydrogen atoms, was found to react in CCl_4 over a period of several days, while the cluster $(H)_2Os_3(CO)_{12}$ containing two terminal hydrides reacted readily with CCl_4, to give the ligand substitution product $Os_3(Cl)_2(CO)_{12}$ presumably via a radical pathway.[3] Norton and co-workers have examined radical chain mechanisms in which the monometallic osmium compound $H_2Os(CO)_4$ acts as both a hydrogen atom source and the radical chain carrier.[4] While a number of studies have measured proton transfer rates, and qualitative studies have revealed the participation of radical pathways in ligand exchange and in reduction of haloalkanes for osmium hydrides, no work to quantitatively determine the *homolytic* reactivity of the μ-bonded hydrogen has appeared. We now report the reactivity of the five triosmium clusters $Os_3(\mu\text{-}H)_2(CO)_9\text{-}PPh_3$ (**1**), $Os_3(\mu\text{-}H)(H)(CO)_{10}PPh_3$ (**2**), $Os_3(\mu\text{-}H)(CO_9)(\mu_3\text{-}\eta^2\text{-}C_9H_6N)$ (**3**), $Os_3(\mu\text{-}H)(CO_9)(\mu\text{-}\eta^2\text{-}C_9H_6N)PPh_3$ (**4**), and $Os_3(\mu\text{-}H)(CO_{10})(\mu\text{-}\eta^2\text{-}C_9H_6N)$ (**5**) toward hydrogen abstraction by benzyl radicals.

[†] Pacific Northwest National Laboratory.

[‡] University of Montana.

(1) Dedieu, A. *Transition Metal Hydrides*; VCH: New York, 1992. Hlatky, G. G.; Crabtree, R. H. *Coord. Chem. Rev.* **1985**, *65*, 1. Pearson, R. G. *Chem Rev.* **1985**, *85*, 41. Sweany, R. L.; Halpern, J. *J. Am. Chem. Soc.* **1977**, *99*, 8335.

(2) Bullock, R. M. *Comments Inorg. Chem.* **1991**, *12*, 1. Eisenberg, D. C.; Norton, J. R. *Isr. J. Chem.* **1991**, *31*, 55.

(3) (a) Johnson, B. F. G.; Lewis, J.; Kilty, P. A. *J. Chem. Soc. A* **1968**, 2859. (b) Cook, N.; Smart, L.; Woodward, P. *J. Chem. Soc., Dalton Trans.* **1977**, 1744. (c) Moss, J. R.; Gram, W. A. *J. Chem. Soc., Dalton Trans.* **1977**, 89. (d) Kaesz, H. D.; Saillant, R. D. *Chem Rev.* **1972**, *72*, 248.

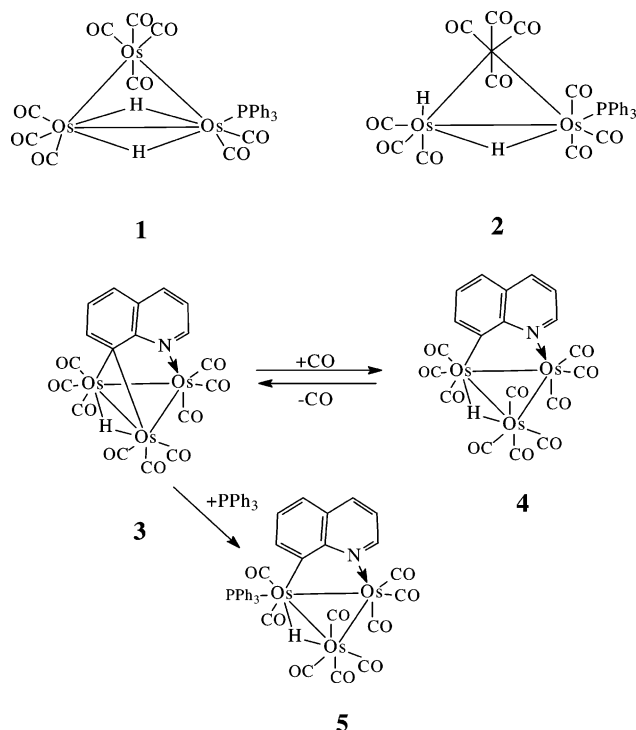(4) Norton, J. R.; Edidin, R. T. *J. Am. Chem. Soc.* **1986**, *108*, 948.

Figure 1. Structures of hydrogen donors.

Structural Characteristics of Compounds 1, 2, and 3

The clusters (Figure 1) chosen for this study contain hydrides in distinctly different bonding modes and provide an opportunity to examine the effect of structural and electronic differences on the absolute rate constants for hydrogen abstraction.

$Os_3(\mu\text{-}H)_2(CO)_9PPh_3$ (**1**)[5] is an electron-deficient (46e$^-$) cluster containing two bridging hydrides along the same Os–Os bond. $Os_3(\mu\text{-}H)(H)(CO)_{10}PPh_3$ (**2**)[5] is an electron-precise (48e$^-$) triosmium cluster containing both a bridging and terminal hydride. The two hydrides of **2** are observed as two signals in the low-temperature limit by ^1H NMR spectroscopy.[6] These signals merge at room temperature since the hydrides are exchanging rapidly on the NMR time scale. The third cluster, $Os_3(\mu\text{-}H)\text{-}(CO)_9(\mu_3\text{-}\eta^2\text{-}C_9H_6N)$ (**3**),[7] contains a quinoline ring bound to the cluster at the C(8) position by a three-center two-electron bond along the same edge of the cluster as the μ-H hydride and coordination of the nitrogen lone pair at the remaining osmium, resulting in an electron-deficient 46e$^-$ cluster. The aromaticity of the quinoline ring remains unperturbed. Electrochemical studies have suggested that radical formation is likely to occur at the metal core after hydrogen atom abstraction by benzyl radical.[8] Compound **3** reacts rapidly with carbon monoxide to give compound **4**.[7] Decarbonylation of compound **4**, by photochemical or thermal dissociation, results in
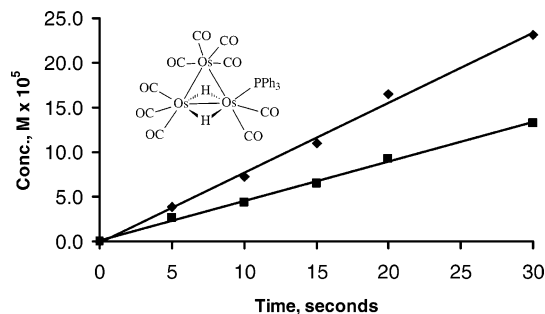
(5) (a) Deeming, A. J.; Hasso, S. J. *J. Organomet. Chem.* **1975**, *88*, C21. (b) Shapley, J. R.; Keister, J. B.; Churchill, M. R. *J. Am. Chem. Soc.* **1975**, *97*, 4145. (c) Deeming, A. J.; Hasso, S. J. *J. Organomet. Chem.* **1976**, *114*, 313.

(6) Rosenberg, E.; Anlsyn, E. V.; Barner-Thorsen, C.; Aime, S.; Osella, D.; Gogetto, R.; Milone, L. *Organometallics* **1984**, *3*, 1790.

(7) Kabir, S. E.; Kolwaite, D. S.; Rosenberg, E.; Hardcastle, K.; Cresswell, W.; Gringstaff, J. *Organometallics* **1995**, *14*, 3611.

(8) Arcia, E.; Kolwaite, D. S.; Rosenberg, E.; Hardcastle, K.; Ciurash, J.; Duque, R.; Osella, D.; Gogetto, R.; Milone, L. *Organometallics* **1998**, *17*, 415.

Figure 2. Time-dependent production of toluene (◆) and bibenzyl (■) during the photolysis of a solution containing **1** (3.8×10^{-3} M) and dibenzyl ketone (1.00×10^{-2} M) in benzene at 25 °C. The linearity of bibenzyl and toluene formation reflects a constant rate of formation of benzyl radical and negligible (<5%) consumption of donor.

the re-formation of compound **3**. The reaction of compound **3** with triphenylphosphine results in coordination of the phosphine followed by carbonyl migration to give compound **5**.[7] The electron-precise compound **5** does not lose carbon monoxide upon photolysis or thermolysis.[7] Clusters **1** and **2** were chosen in this study because they are ideal for comparison of radical abstraction rates for bridging versus terminal hydrides. Compounds **3**, **4**, and **5** provide insight into the differences in the relative reactivity of hydrides on saturated (48e$^-$) and unsaturated (46e$^-$) clusters. In addition to the electronic effects, the steric effects on hydrogen abstraction can be probed with this set of clusters when the rates from **4** and **5** are compared.

Results and Discussion

Rate constants for the benzyl radical abstraction from osmium hydrides, **1**–**5**, were determined by a competition of hydrogen atom abstraction to form toluene with benzyl radical self-termination to form bibenzyl. The photolysis of dibenzyl ketone (DBK) provides a readily accessible source of benzyl radicals, eq 1.

$$PhCH_2C(O)CH_2Ph \xrightarrow{h\nu} 2PhCH_2{}^\bullet + CO \qquad (1)$$
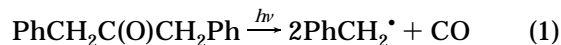
Rate constants were determined in competition kinetic experiments that measure the rate of formation of toluene form benzyl radical in competition with self-termination of benzyl radical to form bibenzyl. The method has been described in detail previously.[9] Under constant rate of photolysis of DBK and low conversion of the hydrogen atom donor the relationship between toluene, bibenzyl, and the average hydrogen atom donor concentration, [donor]$_{av}$, where [donor]$_{av}$ = ([donor]$_{initial}$ + [donor]$_{final}$)/2 = (2[donor]$_{initial}$ − [toluene])/2 over a period of photolysis time, Δt in seconds, is given by eqs 2a–d. Under conditions where benzyl radical concentration and donor concentration are constants, eqs 2a and 2b may be integrated. Division of the integral of eq 2a by the square root of the integral of eq 2b yields eqs 2c and 2d. Equations 2a and 2b predict linear production of toluene and bibenzyl for constant benzyl and donor concentrations, as observed (cf. Figure 2).

(9) Franz, J. A.; Linehan, J. C.; Birnbaum, J. C.; Hicks, K. W.; Alnajjar, M. S. *J. Am. Chem. Soc.* **1999**, *121*, 9824.

$$\frac{d[\text{toluene}]}{dt} = k_{\text{abs}}[\text{benzyl}][\text{donor}] \qquad (2a)$$

$$\frac{d[\text{bibenzyl}]}{dt} = k_t[\text{benzyl}]^2 \qquad (2b)$$

$$\frac{[\text{toluene}]}{[\text{bibenzyl}]^{1/2}} = \frac{k_{\text{abs}}[\text{donor}]\Delta t}{k_t^{1/2}\Delta t^{1/2}} \qquad (2c)$$

$$k_{\text{abs}} = \frac{[\text{toluene}]k_t^{1/2}}{[\text{bibenzyl}]^{1/2}[\text{donor}]_{\text{av}}\Delta t^{1/2}} \qquad (2d)$$

In previous work, we determined absolute rate expressions for the reaction of benzyl radical with Bu₃SnH, PhSH, Cp*Mo(CO)₃H, and DCPH (dicyclohexylphosphine) versus self-termination of the benzyl radical ($k_{\text{abs}}/k_t^{1/2}$).[9,10] An accurate procedure that employs the Spernol–Wirtz/Debye–Einstein/Smoluchowski (SW) description of self-termination rates of small organic radicals in nonassociating solvents was evaluated by Fischer and co-workers for comparison with extensive ESR[11] and optical spectroscopic[12] rates of self-termination reactions. The SW procedure[9] for prediction of self-termination rates is applied in the present work. Equation 2d is valid under conditions of short extent of conversion of hydride donor and a constant rate of benzyl radical formation from DBK photolysis. These conditions are verified by plots of [toluene] and [bibenzyl] versus time. Figure 2 shows a typical plot obtained during the photolysis of a solution containing compound **1** (3.8×10^{-3} M) and dibenzyl ketone (1.00×10^{-2} M) in benzene at 25 °C. The plot demonstrates constant rate of production of benzyl radical concentration at low donor consumption (<5%).

Thus, the benzyl radical self-termination constant, $2k_t$, is calculated at each temperature using the temperature-dependent rate expression $\ln(2k_t/\text{M}^{-1}\,\text{s}^{-1}) = 27.23 - 2952.5/RT$, RT in cal/mol, estimated using the Debye/Einstein/Smoluchowski equation employed in previous work.[9,12] The use of eq 2 to obtain k_{abs} yields less than 20% error in k_{abs} in the rate constant with donor conversions of up to 50%. In this study, the donor consumption was kept below about 7%, yielding negligible error from this source. Table 1 presents rate parameters for abstraction by benzyl radical from the donors Os₃(μ-H)₂(CO)₉PPh₃ (**1**), Os₃(μ-H)(H)(CO)₁₀PPh₃ (**2**), Os₃(μ-H)(CO₉)(μ_3-η^2-C₉H₆N) (**3**), Os₃(μ-H)(CO₁₀)-(μ-η^2-C₉H₆N) (**4**), and Os₃(μ-H)(CO₉)(μ-η^2-C₉H₆N)PPh₃ (**5**). The values of k_{abs} were obtained by GC analysis of the mixtures of toluene and bibenzyl after photolysis. The results are a combination of several initial donor concentrations and at least four temperatures.

Due to the symmetrical nature of the hydrides in compound **1**, the initial donor concentration was multiplied by 2 in eq 2 to give rate constants on a per-hydrogen basis. Plots of $\ln(k_{\text{abs}})$ versus $1/T$ for the reaction of benzyl radical and compound **1** are linear up to 100 °C. The complexes exhibit decomposition above 100 °C; thus kinetics were restricted to temperatures at which the complexes were found to be stable over the photolysis lifetimes. Compound **1** has been shown to react readily with CO to form Os₃(μ-H)(H)(CO)₁₁,[13] which contains both a bridging and a terminal hydride, and is analogous in structure to compound **2** of this study. The photolysis of dibenzyl ketone and the thermal decomposition of donor radical species are potential sources of carbon monoxide that could react with compound **1** to form Os₃(μ-H)(H)(CO)₁₁. Thus, higher temperatures and significant products of CO from photolysis of dibenzyl ketone were avoided.

Studies of the fluxional motion of compounds isostructural with compound **1** have shown that no exchange occurs between the bridging hydrides even at elevated temperatures.[6] While intramolecular carbonyl exchange in Os₃(CO)₁₀(μ-H)₂ occurs through a simple pinwheel motion, it is not accommodated with motion of the bridging hydrides (i.e., no deuterium kinetic isotope effect was observed between Os₃(μ-H)₂(CO)₁₀ and Os₃(μ-D)₂(CO)₁₀).[6] ¹H NMR data for **1** do not reveal detectable resonances of terminal hydride. The lack of detectable terminal hydride, together with the slow hydrogen exchange rate, suggests that terminal hydride structure is not present in appreciable concentrations and is unlikely to be acting as a donor.

Compound **2**, containing both a terminal and bridging hydride, was found to be much more reactive toward hydrogen abstraction. Figure 3 presents a comparison of the Arrhenius plots of hydrogen abstraction from **2** and **1** by benzyl radical. The rate of hydrogen atom abstraction from compound **2** calculated from experimental data is approximately 30 times faster at room temperature than the rate for compound **1**. This difference in reactivity may not necessarily be attributed to any difference in bond strength. The difference between terminal and bridging hydride bond strengths has been shown to be within a range of 0–5 kcal/mol for a large variety of transition metal complexes with an average bond strength of around 60 kcal/mol.[14] The difference in reactivity between compounds **1** and **2** is more likely due to greater kinetic accessibility of the terminal hydride in compound **2** and the electron-deficient nature of compound **1**. Structural studies on compound **1** have shown the terminal Os–H bond length to be 1.52 Å and the average bridging hydride bond lengths to be 1.87 Å, with a slight elongation of the bond between the non-phosphine-coordinated osmium and the bridging hydride.[15a] The interpretation of the reactivity in terms of Os–H bond lengths is limited by the lack of more accurate neutron diffraction M–H bond measurements.[15b] The PPh₃ ligand is also in a position to sterically hinder the approach of the benzyl radical to the bridging hydride in **1**, further reducing its reactivity.

Direct location of the hydrides in compound **1** has not been accomplished, but studies on the isostructural complex Os₃(μ-H)₂(CO)₁₀ showed symmetrical bridging hydrides with a Os–H bond length of 1.85 Å.[16] The bond

(10) Franz, J. A.; Suleman, N. K.; Alnajjar, M. S. *J. Org. Chem.* **1986**, *51*, 19.

(11) Lehni, M.; Schuh, H.; Fischer, H. *Int. J. Chem. Kinet.* **1979**, *11*, 705.

(12) (a) Claridge, R. F.; Fischer H. J. *J. Phys. Chem.* **1983**, *87*, 1960. (b) Huggenberger, C.; Fischer, H. J. *Helv. Chem. Acta* **1981**, *64*, 338.

(13) Shapley, J. R.; Keister, M. R.; Churchill, M. R.; DeBoer, G. *J. Am. Chem. Soc.* **1975**, *97*, 4145.

(14) (a) Stevens, A. E.; Beauchamp, T. L. *J. Am. Chem. Soc.* **1981**, *103*, 190. (b) Pearson, R. G. *Chem. Rev.* **1985**, 41.

(15) (a) Churchill, R.; DeBoer, B. G. *Inorg. Chem.* **1977**, *9* (16), 2397. (b) See, e.g.: Bau, R.; Drabnis, M. *Inorg. Chim. Acta* **1997**, *259*, 27.

(16) Orpen, G.; Rivera, V.; Bryan, E. G.; Pippard, D.; Shelgrick, G. M. *Soc. Chem. Rev.* **1978**, 723.

Table 1. Arrhenius Rate Parameters for the Reaction of Benzyl Radical and Triosmium Donors in Benzene[a]

donor	$\log(A/M^{-1} s^{-1})$[b]	ΔS^*, cal/mol K	E_a, kcal/mol[b]	ΔH^*, kcal/mol	T_m, K	k (M^{-1} s^{-1}) 298 K	temp range, K
Os$_3$(μ-H)$_2$(CO)$_9$PPh$_3$, **1**	9.40 ± 0.3	-17.4	8.11 ± 0.5	7.44	335	2.8×10^3	297–373
Os$_3$(μ-H)(H)(CO)$_{10}$PPh$_3$, **2**	8.08 ± 0.3	-23.4	4.32 ± 0.3	3.66	332	8.2×10^4	297–363
Os$_3$(μ-H)(CO)$_9$(μ_3-η^2-C$_9$H$_6$N), **3**	10.1 ± 2	-14.2	10.50 ± 3	9.84	330	2.5×10^2	298–363
Os$_3$(μ-H)(CO)$_9$(μ-η^2-C$_9$H$_6$N)PPh$_3$, **5**	7.0 ± 0.5	-28.5	4.25 ± 0.7	3.59	333	7.1×10^3	313–367
Os$_3$(μ-H)(CO)$_{10}$(μ-η^2-C$_9$H$_6$N), **4**[c]	nd		nd			$5 \pm 2 \times 10^4$	297

[a] Errors are 2σ. [b] Arrhenius parameters A and E_a, $k = Ae^{-E_a/RT}$, are described by $A = (ekT_m/h) \exp(\Delta S^*/R)$ and $E_a = \Delta H^* + RT_m$, where e is the base of natural logarithms, k is Boltzmann's constant, T_m is the mean temperature of the experiments, and h is Planck's constant. [c] Temperature-dependent rate constants could not be determined for this compound due to CO loss at elevated temperatures.
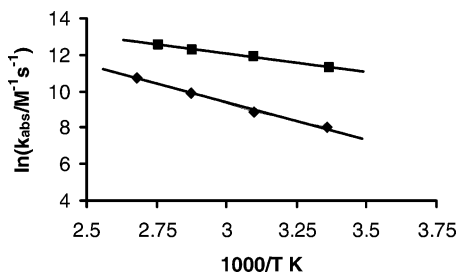

Figure 3. Arrhenius plots for hydrogen abstraction by benzyl radical from Os$_3$(μ-H)$_2$(CO)$_9$PPh$_3$, **1** (◆), and Os$_3$(μ-H)(H)(CO)$_{10}$PPh$_3$, **2** (■), in benzene. Each data point represents the average of 3–6 experiments (see Experimental Section).

lengths of the bridging hydrides in compounds **1** and **2** are nearly identical. However, bond lengths are not necessarily indicators of bond energies, and the overall electronic state of both complexes (46e$^-$ and 48e$^-$ clusters, respectively) may play a significant role in the reactivity of both the bridging and terminal hydrides. The electron deficiencies of compound **1** may result in a reduction of the reactivity of the bridging hydrides toward hydrogen abstraction. In **2** the k_{abs} rate of the terminal hydride was assumed to far exceed (by a factor of at least 10) the k_{abs} rate of the doubly bridging compound. Bridge–terminal exchange is occurring in compound **2** at room temperature. The rate of bridge–terminal exchange at 298 K is 2.2×10^3 s^{-1} (extrapolated from low-temperature NMR studies),[6] which is 40 times slower than the rate of hydrogen abstraction at 298 K, indicating that the incoming benzyl radical is not reacting with the diterminal hydride transient intermediate species.

The room-temperature rate of hydrogen abstraction, $k_{abs} = 2.5 \times 10^2$ M^{-1} s^{-1}, by benzyl radical from compound **3**, which contains a bridging monohydride, was slower, by at least a factor of 10, than hydrogen abstraction from compound **1** and is approaching the limit of detection by this kinetic method. (The toluene formed by abstraction from the metal hydride, **3**, is about 3 times greater than the background toluene concentration of the triply distilled benzene.) Thus, this k_{abs} value is close to the lowest value measurable by the abstraction/termination competition kinetic method. Both **1** and **3** are electron deficient, but compound **1** is much less sterically hindered for radical attack. The quinoline ring of compound **3** blocks an entire face of the cluster and may be responsible for the dramatic decrease in reactivity. In a previous study we have shown that steric hindrance of both the metal hydrogen atom donor and the incoming alkyl radical is responsible

for significant rate differences, even for a highly exothermic reaction.[9]

The rate of hydrogen atom donation dramatically increases upon addition of another ligand to **3** due to an increase in electron density on the metal cluster. The room-temperature rate constant for compound **5**, which contains an added triphenylphosphine ligand, approaches that obtained for **2** and is 3 times faster than for **1**. The room-temperature rate constant for **4**, which contains an added carbon monoxide ligand, is one of the fastest obtained in this study. Both **4** and **5** are 48e$^-$ complexes as opposed to **3** and **1**. While the rate differences between the compounds used in this study are certainly sensitive to steric effects, we note that a cluster that is *more* sterically hindered (**5** vs **3**) is the more reactive. While the overall observed abstraction rates involve the convolution of steric, electronic, and enthalpic effects, the present results are at the least suggestive of higher reactivity for the complexes with greater coordinative saturation. In addition, smaller ligands on complexes with similar electron densities yield faster rates of hydrogen atom abstraction. This is best illustrated when **4** is compared with **5**. Even though triphenylphosphine is a better electron donor than carbon monoxide, the rate of hydrogen abstraction is much higher for **4** than for **5**. Since the added ligand ends up on an osmium that also contains the bridging hydride, the steric considerations must be considered; see Figure 1. The smaller steric bulk of carbon monoxide when compared to triphenylphoshine leads to the 5-fold increase in rate.

Another possible explanation of the rate difference between the phosphine and the carbon monoxide addition complexes **4** and **5** is the possible enhanced stabilization of the complex after hydrogen atom loss by carbon monoxide. The carbon monoxide ligand may stabilize the cluster resulting from hydrogen atom loss through its ability to bridge multiple metal centers. Finally it should be pointed out that in **3** the bridging hydrides are tucked below the plane of the Os$_3$ triangle, while in **4** the bridging hydride is in the plane, making it more accessible to abstraction since it is somewhat less hindered by the surrounding carbonyl groups.[7,8]

The activation barriers shown in Table 1 support the observation that clusters with higher electron densities donate their hydrogen atoms more easily than clusters with lower electron densities. The activation barriers for hydrogen atom abstraction by both of the electron-deficient clusters **1** and **3** are greater than 8 kcal/mol, while those for the electron-rich clusters **2** and **5** are approximately 4 kcal/mol. Unfortunately, complex **4** thermally and photochemically loses the carbon mon-

oxide ligand in competition with hydrogen abstraction, so any temperature-derived parameters such as activation energies cannot be obtained. (If a conventional Arrhenius A-factor of $10^{8.5}$ M^{-1} s^{-1} is assigned to **4**, an Arrhenius activation energy of 5.2 kcal/mol is estimated for **4**.)

Conclusions

This work shows that bridging hydrides as well as terminal hydrides are kinetically accessible to abstraction by carbon-centered radicals under relatively mild conditions. Factors affecting the hydrogen donor ability appear to include the degree of coordinative saturation of the cluster as well as the steric hindrance of ancillary ligands. Due to the complex interplay of steric and electronic effects, unambiguous characterization of the effect of coordinative unsaturation on homolytic reactivity of the Os hydrides will await more detailed studies.

Experimental Section

General Procedures. Gas chromatographic analysis was performed on a Hewlett-Packard 5890 Series II equipped with a HP GC splitless injector and a 30 m × 0.25 mm HP-5 high-performance capillary column and a flame-ionization detector.

Reagents. 1,3-Diphenyl-2-propanone (DBK, dibenzyl ketone) was purchased from Aldrich, recrystallized four times from hexane at −25 °C (>99.9% purity, free of toluene and bibenzyl), and stored in the dark at −25 °C. Benzene was purchased from Aldrich and fractionally distilled three times to remove trace quantities of toluene. Toluene, bibenzyl, and *tert*-butylbenzene were purchased from Aldrich and used without further purification. Os₃H₂(CO)₉PPh₃ (**1**),[5] Os₃(μ-H)(H)(CO)₁₀PPh₃ (**2**),[5] Os₃(μ-H)(CO)₉(μ_3-η^2-C₉H₆N) (**3**),[7] Os₃(μ-H)(CO)₁₀(μ-η^2-C₉H₆N) (**4**),[7] and Os₃(μ-H)(CO)₉(μ-η^2-C₉H₆N)PPh₃ (**5**)[7] were synthesized as previously reported and recrystallized in CH₂Cl₂/hexane at −25 °C.

GC Standardization. A stock solution of 1.00×10^{-4} M, toluene, bibenzyl, and *tert*-butylbenzene in benzene was further diluted with a stock solution of 1.00×10^{-4} M *tert*-butylbenzene in benzene, to concentration ranges between 5.00×10^{-7} and 5.00×10^{-5} M. Plots of GC peak area ratios (analyte/*tert*-butylbenzene) versus molarity ratios (analyte/*tert*-butylbenzene) yield linear plots over this concentration range.

Photolysis of Dibenzyl Ketone in the Presence of Os₃-(μ-H₂)(CO)₉PPh₃ (1). Samples from a stock solution of 1.00×10^{-2} M dibenzyl ketone, 1.00×10^{-4} M *tert*-butylbenzene (internal GC standard), and Os₃(μ-H₂)(CO)₉PPh₃, 3.8×10^{-3} M, in benzene, were freeze−thaw-degassed with three cycles and sealed in 5 mm diameter quartz tubes for photolysis. The samples were photolyzed in a HP 5710A GC oven equipped with a quartz window, for temperature control. The light source was a Hanovia high-pressure Xe arc lamp powered by a Spectral Energy LPS5255HR arc lamp power supply. The

light was passed through a water infrared filter and was focused at a 2.0 cm diameter target area. The time of photolysis was controlled by a Uniblitz model 225L0A0T522952 computer-controlled electronic shutter. The samples were photolyzed at 337 nm for 3−35 s (±0.25 s) at 25, 50, 75, and 100 °C (±0.5 °C), with less than 1% consumption of ketone and less than 7% consumption (in most experiments less than 4%) of donor, to maintain a constant concentration and distribution of radical species. GC analysis of unphotolyzed samples was performed prior to each kinetic run to establish background concentrations of toluene and bibenzyl. Samples were opened in air, and toluene and bibenzyl concentrations were determined by GC. The linearity of production of bibenzyl and toluene with time was confirmed by photolyzing samples for 3, 5, 7, 10, 15, 20, 25, and 30 s. Least-squares treatment of the concentrations of toluene and bibenzyl versus time gave excellent linear correlations and near zero intercepts. Short photolysis times were used to ensure that the buildup of light-absorbing organometallic products was sufficiently low, so that irradiation intensity varied by less than 5% from the front to the back of the sample and a constant radical concentration was maintained. The photolysis was repeated for hydride donor concentrations of 3.8×10^{-4}, 1.28×10^{-3}, and 1.74×10^{-3} M. Photolysis of DBK with compounds **2**−**5** was performed similarly except due to the relatively low k_{abs} rate from compound **3**, it was necessary to correct for trace background toluene not related to hydrogen abstraction from the donor. In this case samples from a stock solution of 1.00×10^{-2} M DBK and 1.00×10^{-4} M *tert*-butylbenzene (internal GC standard) in benzene were photolyzed for 0−60 s and analyzed for toluene and bibenzyl at 25, 50, and 90 °C. Toluene concentrations observed in the presence of **3** were corrected for residual toluene present in triply distilled benzene.

Density and Vapor Pressure Corrections. The density of benzene was calculated at each experimental temperature used. Least-squares fit of density verses T (degrees K) for benzene: $\rho = 1.192 - 0.001059\,T$ where ρ = density of benzene at temperature T (degrees K). Donor and product concentrations were corrected for density effects using the density correction factor = ρ_T/ρ_{298K}. The vapor pressure of benzene was calculated at each experimental temperature using log $P = -(0.05223a/T + b)$.[17]

Supporting Information Available: Tables of the kinetic data for each photolysis are available. This material is available free of charge via the Internet at http://pubs.acs.org.

(17) Reid, R. C.; Prausnitz, J. M. Sherwood, T. K. *The Properties of Liquids and Gases*; MacGraw-Hill: New York, 1977. Weast, R. C.; Astle, M. J. *CRC Handbook of Chemistry and Physics*; CRC Press: Boca Raton, FL, 1982−83.